Sheffield Hallam University

TEM observations of wear mechanisms of TiAlCrN and TiAlN/CrN coatings grown by combined steered-arc/unbalanced magnetron deposition

LUO, Quanshun <http://orcid.org/0000-0003-4102-2129>, RAINFORTH, W.M. and MÜNZ, W.D.

Available from Sheffield Hallam University Research Archive (SHURA) at:

https://shura.shu.ac.uk/26064/

This document is the Accepted Version [AM]

Citation:

LUO, Quanshun, RAINFORTH, W.M. and MÜNZ, W.D. (1999). TEM observations of wear mechanisms of TiAlCrN and TiAlN/CrN coatings grown by combined steered-arc/unbalanced magnetron deposition. Wear, 225-22 (I), 74-82. [Article]

Copyright and re-use policy

See http://shura.shu.ac.uk/information.html

Sheffield Hallam University Research Archive
http://shura.shu.ac.uk

TEM observations of wear mechanisms of TiAlCrN and TiAlNrCrN coatings grown by combined steered-arcrunbalanced magnetron deposition

Q. Luo[a], W.M. Rainforth[a]*, W.-D. Munz[b]

[a] Department of Engineering Materials, University of Sheffield, Mappin Street, Sheffield, S1 3JD, UK

[b] Materials Research Institute, Sheffield Hallam University, Pond Street, Sheffield, S1 1WB, UK

Abstract: The dry sliding wear of monolayer TiAlCrN and TiAlCrYN and multilayer TiAlN/CrN coatings has been investigated against a BM2 tool steel counterface using a ring on block configuration at 91 N, 0.42 m/s. The coatings were deposited on a BM2 tool steel substrate by combined steered-arc/unbalanced-magnetron deposition. The wear rate of the multilayer was superior to the monolayer, although both provide a substantial improvement compared with the wear behaviour of the base BM2 tool steel e.g., wear rate = 6.1×10^{-4} mm^3/m for the BM2 tool steel; 3.98×10^{-5} mm^3/m for the TiAlCrN monolayer and 2.58×10^{-5} mm^3/m for the TiAlNrCrN multilayer. Wear of the coatings occurred by several mechanisms, fine scale -200 nm. detachment in the early stages and micron scale detachment associated with cracking in the coating in the later stages. Detailed transmission electron microscopy of cross-sections of the worn surface indicated that two dominant types of cracking were present within the coating: 1. cracking perpendicular to the coating surface, often along columnar grain boundaries, typically running through the entire coating; 2. cracking approximately parallel to the worn surface, extending across several columnar grains. For the multilayers, there was no evidence that the spalling was induced by decohesion along
the interface of the multilayers. Limited surface deformation was detected at the worn surface of the TiAlCrYN and TiAlCrN, but not at the worn surface of the TiAlNrCrN, tested under identical conditions. In contrast, the uncoated BM2 tool steel worn surface exhibited extensive plastic deformation. The relationship between wear mechanism and coating structure is discussed.

Key Words: TEM observations; TiAlNrCrN coatings; Magnetron deposition

1. Introduction

Physical vapour deposition PVD. nitride coatings possess high hardness and good chemical stability [1–3]. The family of titanium nitride coatings has been developed in three generations. The first generation, TiN deposited as a monolayer, have received widespread commercial use [4,5]. The second-generation coatings were developed by introducing alloy additions to TiN, the most important being TiAlN [6–8] and TiAlCrN [9,10], which have superior oxidation and wear resistance to TiN [6,11]. These coatings often have higher hardness than the first generation and with the addition of Y to TiAlN [12] and TiAlCrN [9], oxidation resistance is also substantially improved. The third generation comprise both multi-component constituents and, importantly, a multilayered structure [13,14]. Multilayer coatings, which have a superlattice structure [15,16], have exceptionally high hardness often referred toas ‘super-hard’. and good thermal and chemical stability.

PVD coatings can be grown by a number of techniques [3], including low voltage electric beam evaporation, triode high voltage electric beam evaporation, cathodic arc evaporation, and magnetron sputtering, each of which have a number of advantages and disadvantages, discussed elsewhere [5,17–19]. The combined cathodic arc etching and unbalanced magnetron sputtering technique [18,19] provides the advantages of enhanced adhesion strength of metallic ion etching and the uniform and effective film growth of unbalanced magnetron sputtering. This technique, used to produce the coatings in the current work, is now being used in fabrication of commercial coatings as well as laboratory development of new coatings [20].

PVD hard coatings are used to enhance the wear resistance of many tribological materials, particularly those operating in severe environments, such as cutting tools [1,4,6,20,21]. The third-generation coatings are sufficiently hard, thermally stable and oxidation resistant that it is believed that they may be able to operate in unlubricated cutting operations. However, third generation coatings have only recently been developed and therefore little is known about their tribological properties. A detailed understanding of the wear mechanisms is required in order to optimize microstructure, and therefore processes variables, for wear resistance. Multilayer coatings are materials engineered on the nanoscale and therefore an understanding of tribological properties requires an understanding of the interaction of stress and environment at this scale. Previous studies have demonstrated that a detailed understanding of the microstructural changes at a worn surface require high magnification transmission electron microscopy TEM studies, with the maximum information being derived from surface cross-sections [22–28]. Accordingly, the present work presents detailed TEM of cross-section from the worn surface of PVD coatings. Second and third generation coatings have been tested under identical conditions and compared with uncoated BM2 tool steel. The present paper reports the TEM findings at a single load and speed, and forms part of a wider study which has investigated the effect of load and speed on the wear mechanism [29].

2. Experimental details

Three coatings were investigated, a multilayer coating, consisting of alternating nanometer thick layers of TiAlN and CrN [14], designated TiAlN/CrN, and two monolayer coatings TiAlCrN and TiAlCrYN [9], all deposited on pre-polished high speed steel BM2. PVD was undertaken in a four target Hauzer HTC1000-ABS coating machine, using the combined cathodic arc etching and unbalanced magnetron sputtering process [18], the full details of which are given elsewhere [9,14,16]. For the TiAlN/CrN coating, the process started with Cr metal ion etching in the steered arc mode, followed by the unbalanced magnetron sputtering deposition for 30 min of a base layer of TiAlN the three TiAl targets, each 50:50 at.% Ti:Al, were operated at 8 kW. The multilayer coating was then deposited with the additional Cr target sputtering at 5 kW and the TiAl targets at 8 kW for 210 min. All four targets are operated in the unbalanced magnetron mode Cr: dual purpose cathode [18].

Table 1 Characteristics of PVD coatings

Coatings	TiAlN/CrN	TiAlCrN	TiAlCrYN
$HK_{0.025}$ (GPa)	29.7 ± 6.1	28.1 ± 4.7	19.4 ± 4.7
Thickness (μm)	3.13 ± 0.05	3.18 ± 0.09	1.89 ± 0.06
Texture ($I_{(111)}$:$I_{(200)}$:$I_{(220)}$)	9.4:1:7.9	1:1.4:1.7	1:3.2:1.3

The deposition parameters for TiAlCrN and TiAlCrYN monolayer coatings were similar to those for the TiAlN/CrN multilayer coating except that the Cr target was operated in the unbalanced magnetron mode continuously at 0.5 kW. The quaternary addition of Y was made by replacing one TiAl target with a TiAl (4 at.% Y). target. For the Y containing coating, a base layer similar to that for the TiAlN/CrN was used to grade the compressive stresses generated by the Y incorporation. Table 1 shows the basic characteristics of the deposited coatings. Unlubricated wear tests were performed in a block-on-ring configuration at room temperature 21°C., using anormal load of 91 N applied by dead weight. and a sliding speed of 0.42 m/s. The coating was applied to the 12 mm diameter flat face of the block. The crowned counterface ring, of diameter 60 mm and width 12 mm, was an uncoated BM2 i.e., the same as the substrate material. Tests were also performed using an uncoated BM2 block. The BM2 tool steel had a Vickers hardness of 7.99±0.08 GPa and a chemical composition given in Table 2. Uncoated samples were metallographically polished to 1 mm diamond prior to testing. Wear rate was determined by measuring the wear scar dimensions using a Vernier attached to an optical microscope accuracy ±0.001mm. Wear rate data was obtained after a total sliding distance of 1000 m. However, the evolution of wear mechanism with time was also investigated by terminating tests at shorter sliding distances.

The worn surface was initially examined in the SEM using a Jeol 6400. Longitudinal cross-section TEM samples were then prepared from all the worn samples, following a procedure described in detail elsewhere [30]. The worn surface was sectioned parallel to the sliding direction

Table 2 Composition of the BM2 steel substrate and counterface

Element	C	Mn	Si	Cr	Ni	Mo	W	V
Content (wt.%)	0.95–1.05	0.15–0.40	0.20–0.45	3.75–4.50	0.3 max	4.5–5.5	5.5–6.75	1.75–2.20

Table 3 Friction and wear properties of PVD coatings and tool steel

Materials	TiAlN/CrN	TiAlCrN	TiAlCrYN	BM2
Average friction coefficient	0.77	0.76	0.71	1.02
Wear rate ($\times 10^{-5}$ mm^3/m)	2.58	3.98	4.32	60.8

using a slow speed saw and mechanically ground using fine grit sizes. to -80 mm. A second surface of the same material and dimensions was then glued to the worn surface with the two samples supported on a Cu grid. Argon ion beam milling to electron transparency was only undertaken from below the worn surface to avoid preferential erosion of the region of interest. The epoxy glue used to bond the two surfaces was retained after ion milling and therefore demonstrated that the extreme worn surface was preserved during thinning. The samples were examined in a Philips 420 operating at 120 kV. and Jeol 3010 operating at 300 kV.

3. Results

The wear rate of coated and uncoated BM2, Table 3, were recorded prior to complete loss of the coating through wear i.e., the wear track was entirely within the coating. Prior wear testing determined the maximum running time before which coating loss occurred and therefore the largest possible wear scar contained entirely within the coating. As seen from Table 3, the multilayer coating exhibited the best wear resistance, although all coatings were substantially superior to the uncoated tool steel. Average friction coefficient was lower for the coatings compared to theBM2, although there was little difference between the coating types.

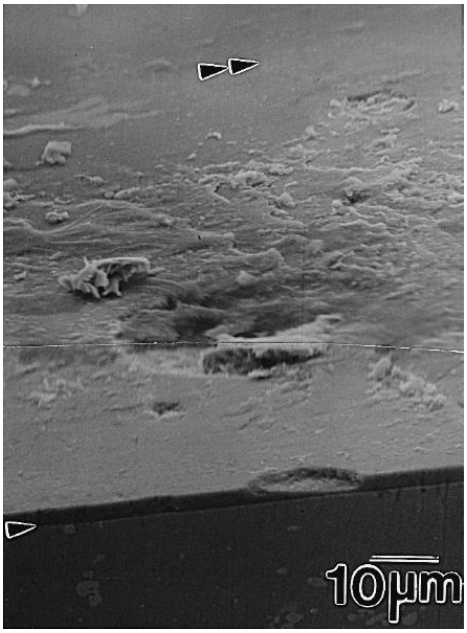

Fig. 1. Scanning electron micrograph of the worn multilayer TiAlN/CrN coating, taken after sectioning the worn surface the substrate/ coating interface is marked by a single arrow and the sliding direction by a double arrow. Note the spalling of the coating. The micrograph clearly demonstrates that the spalling is within the coating and not at the coating substrate interface.

Loss of the coating during the initial stages of wear was caused by spalling Fig. 1. Spalling was from within the coating at this stage, with no evidence of detachment at the coating-substrate interface. The base of the spall had an irregular morphology, but ran approximately parallel to the

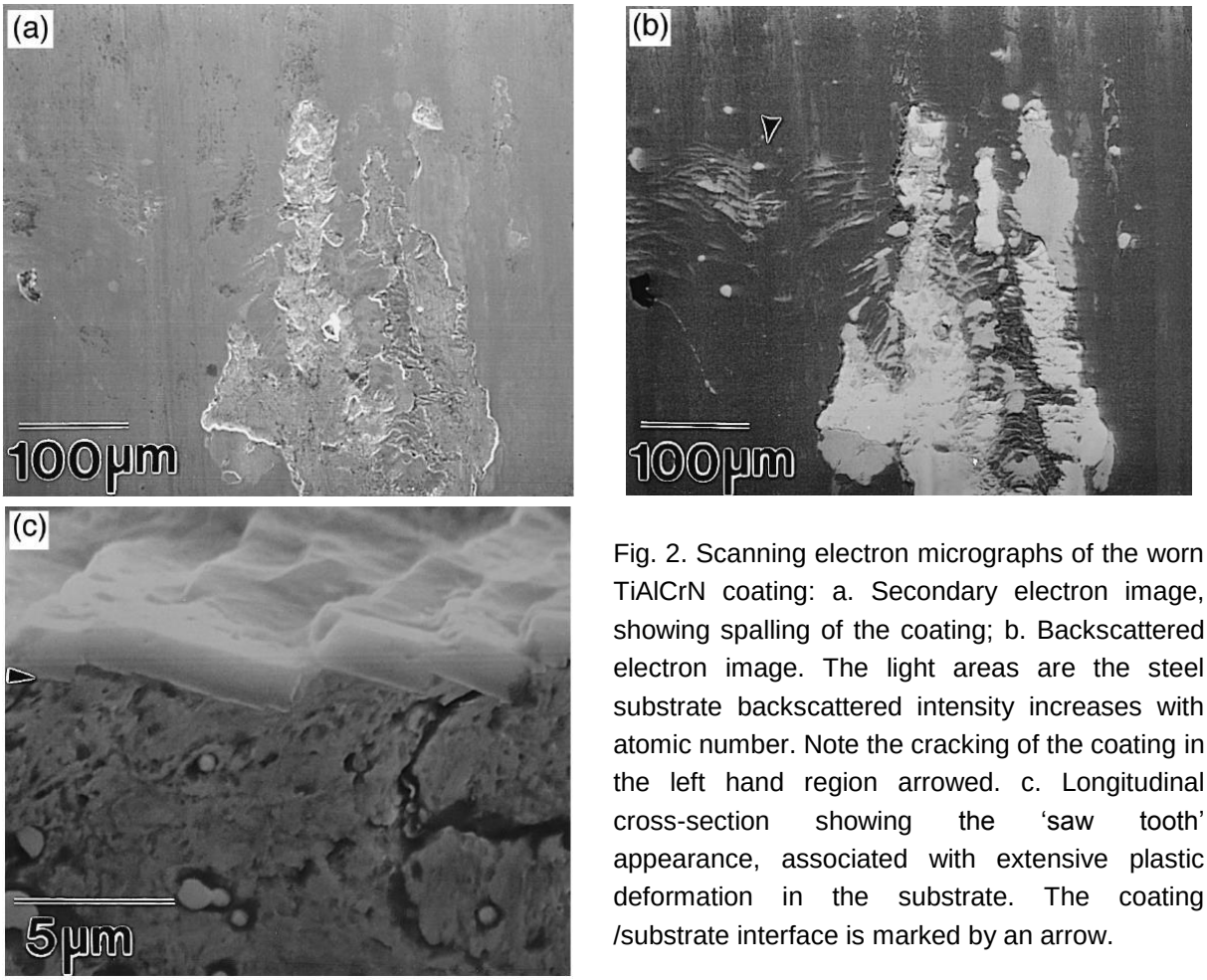

Fig. 2. Scanning electron micrographs of the worn TiAlCrN coating: a. Secondary electron image, showing spalling of the coating; b. Backscattered electron image. The light areas are the steel substrate backscattered intensity increases with atomic number. Note the cracking of the coating in the left hand region arrowed. c. Longitudinal cross-section showing the 'saw tooth' appearance, associated with extensive plastic deformation in the substrate. The coating /substrate interface is marked by an arrow.

coating surface. In contrast, the sides of the spall were generally smooth and perpendicular to the coating surface. In addition to the spalling, thin, irregular surface films were present Fig. 1. Despite the differences in wear rate between the coatings, no obvious differences in worn surface morphology could be detected in the SEM.

Regions of locally dense spalling eventually led to complete loss of the coating and penetration of the counterface through to the BM2 substrate Fig. 2. At this point, wear of the coating at the edge of the wear scar was accelerated. This was associated with extensive cracking within the coating Fig. 2b. Similar gross cracking was observed in the coating just prior to exposure of the substrate and the presence of this cracking indicated the onset of coating failure Fig. 2c. Again, this type of wear mechanism was the same for all coatings tested. The full details of the SEM observations of the coating wear mechanisms as a function of sliding speed and load are given elsewhere [29].

For the TEM observations, samples were removed from the two distinct wear regimes where the wear scar was contained entirely within the coating: 1. the early stages of wear and 2. where gross cracking indicated the onset of coating failure. Fig. 3 gives a low magnification TEM micrograph taken from the TiAlN/CrN multilayer taken from regime 1. This shows no evidence of significant microstructural change either in the coating or substrate note also the excellent bond

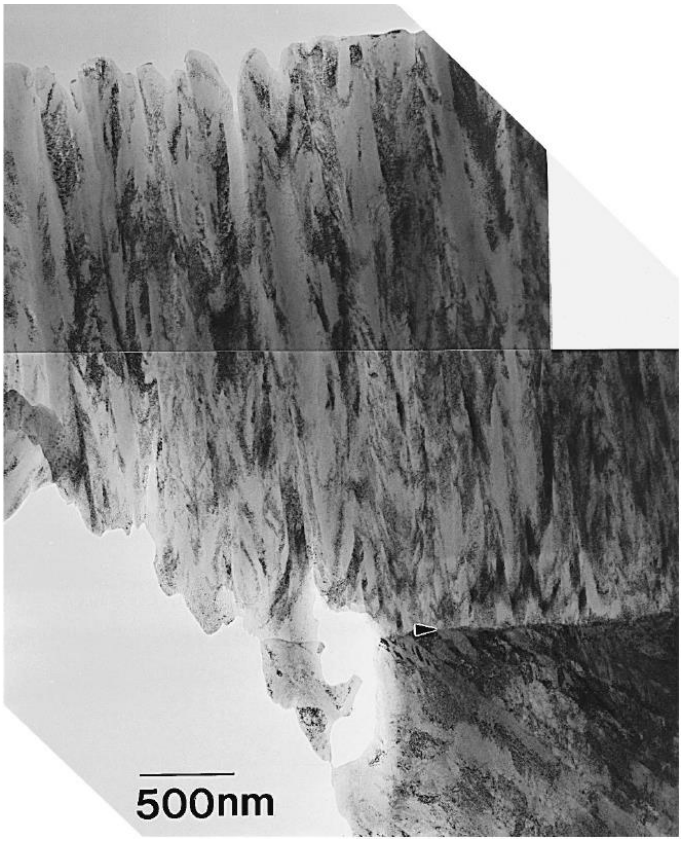

Fig. 3 Bright field TEM micro graph from a longitudinal cross-section sample of the worn TiAlNrCrN multilayer. The sample was taken during the initial stages of wear. The upper left surface has been eroded during ion thinning and is therefore not the original worn surface. Note the general absence of damage either by cracking or deformation. The arrow indicates the direction of sliding and the interface between coating and substrate.

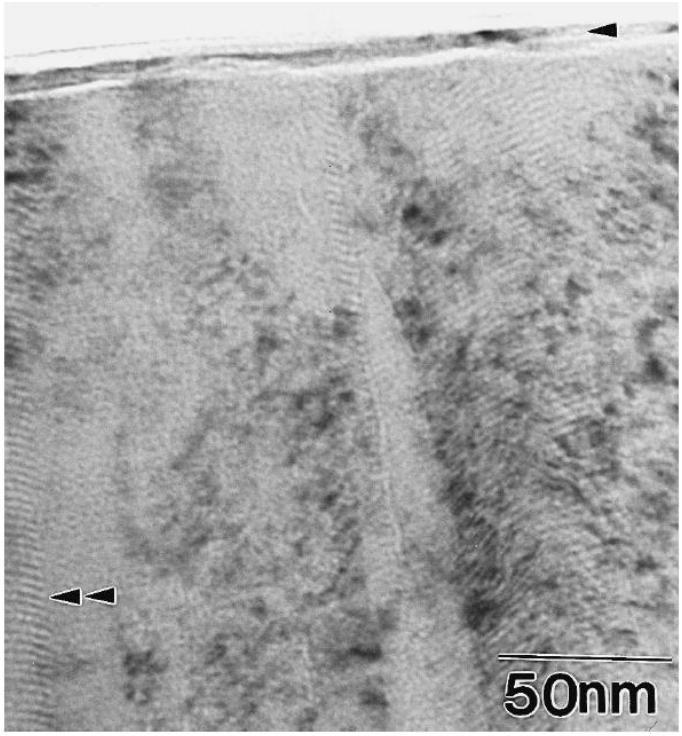

Fig. 4. Bright field TEM micrograph from a longitudinal cross-section sample of the worn TiAlNrCrN multilayer showing the extreme worn surface. A thin surface layer has become detached arrowed. However, detachement did not occur at a layer interface. This feature was not observed on either of the worn monolayer coatings. the multilayer structure can be seen from the Fresnel contrast e.g., at the double arrow. There is a columnar grain boundary running top to bottom at the mid position of the micrograph. The sliding direction is indicated by the direction of the arrows.

between coating and substrate and the columnar structure to the coating. Fig. 4 gives a higher magnification bright field micrograph of the extreme worn surface as labelled by the retention of the epoxy resin. A thin delaminated layer is present of thickness ~8 nm, which was observed at

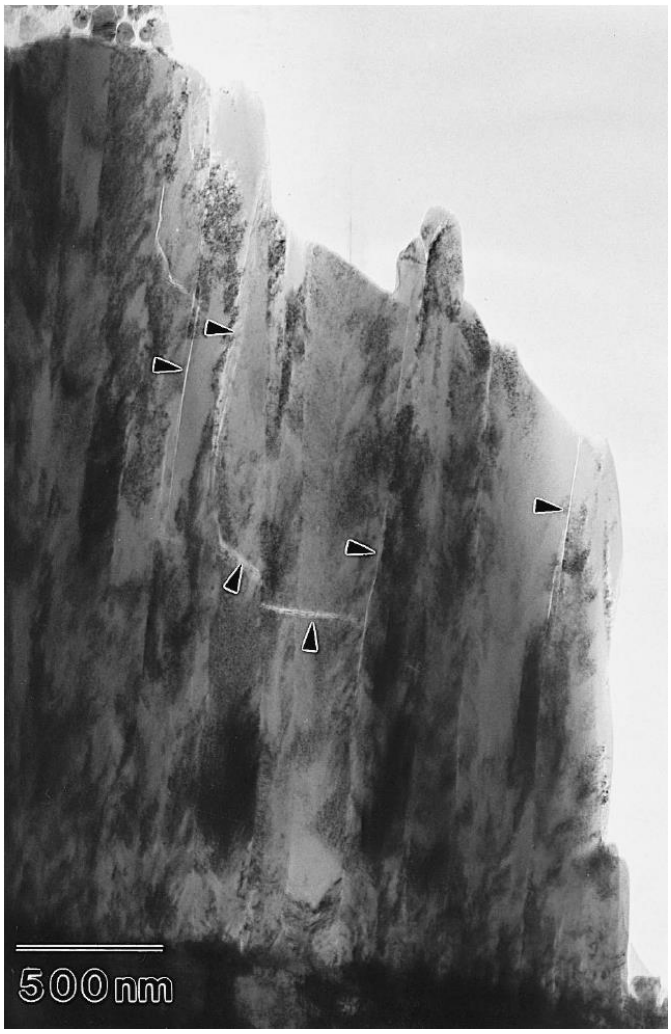

Fig. 5. Bright field TEM micrograph from a longitudinal cross-section sample of the worn TiAlNrCrN multilayer which exhibited damage in regime 2. The parallel cracks arrowed. did not run along the TiAlNrCrN interface, but those perpendicular to the worn surface were
generally along columnar grain boundaries. The interface between substrate and coating corresponds to the position of the scale bar.

several points on the surface. The multilayer structure is evident within this image the image is taken just out of focus to provide Fresnel fringe contrast of the multilayer structure. From which it can be seen that detachment of this layer did not occur along the TiAlN/CrN interface. Interestingly, the multilayer structure appears to be preserved up to the delaminated layer suggesting that frictional heating had not been sufficient to cause breakdown of the layered structure through diffusion.

Fig. 5 gives a bright field TEM image from the edge of the TiAlN/CrN wear scar taken from regime 2., i.e., with the presence of macroscopic cracking which indicated the onset of coating failure. Extensive cracking is apparent within the coating. In this instance, cracking falls into two broad categories: 1. cracking perpendicular to the worn surface, frequently but not always. along the columnar grain boundaries; 2. cracking across the grain boundaries, often within ± 20° to the coating surface. Some of the cracking along columnar grain boundaries was present in the as-deposited state, but its extent was substantially greater after wear testing. Fine wear debris from the TiAlN/CrN identified by selected area electron diffraction. was present at the worn surface Fig. 6.

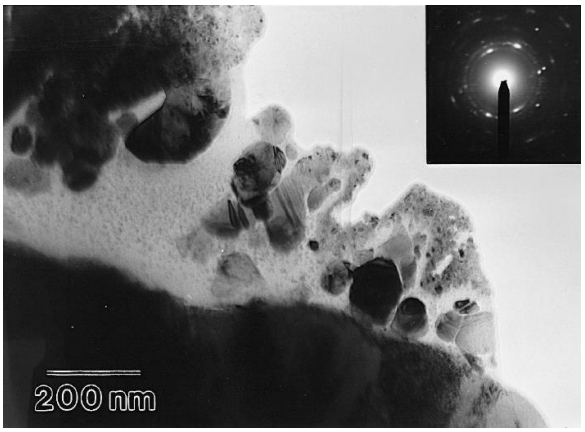

Fig. 6. Bright field TEM micrograph from a longitudinal cross-section sample of the worn TiAlNrCrN multilayer showing wear debris particles at the worn surface.

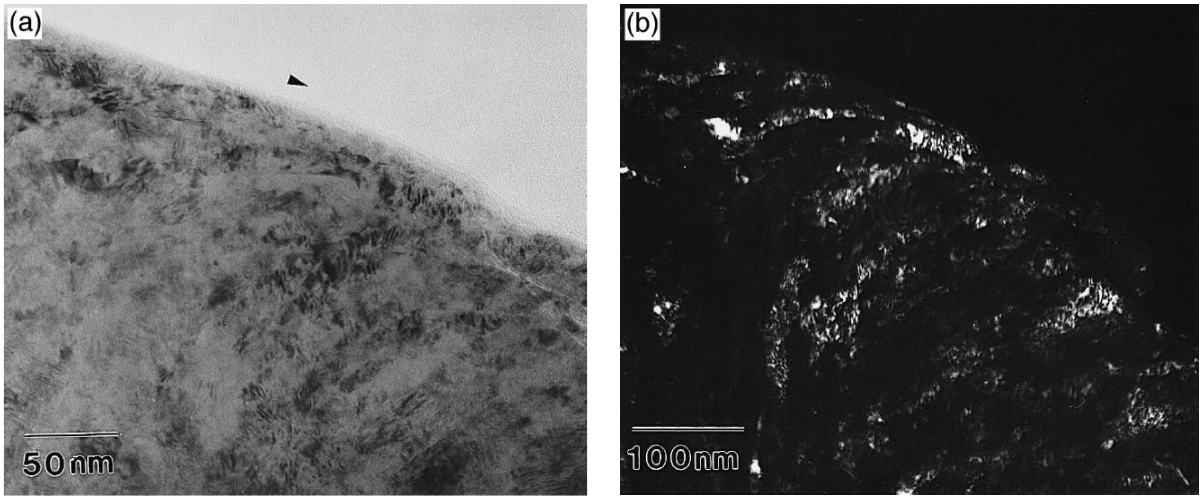

Fig. 7. TEM micrographs from a longitudinal cross-section sample of the worn TiAlCrYN monolayer showing the extreme worn surface. a. Bright field image; b. Dark field image. Note the bending of the structure in the direction of sliding arrowed, indicating surface deformation.

Fig. 7 gives a bright and dark field TEM images of the worn surface of the TiAlCrYN monolayer during the early stages of wear. The dark field image Fig. 7b. indicates abending of the columnar grain structure in the direction of sliding, which is evidence of surface deformation. The depth of deformation as determined by the bending of the columnar structure. varied along the surface in the range ~50-200 nm. Similar deformation was observed for the TiAlCrN, but was never seen at the surface of the TiAlN/CrN multilayer.

Cracking parallel to the surface was observed in the TiAlCrYN sample in several places and was generally located at a depth where the deformation was just visible in the TEM, Fig. 8a. The cracking led to periodic spalling of the deformed layer Fig. 8b.

Fig. 9 gives micrographs from the wear scar of the TiAlCrN in regime 2., i.e., where the coating contained macroscopic cracking. Extensive plastic deformation had occurred in the BM2 substrate. The coating had fractured extensively, with a regular displacement of both coating and substrate, giving a ‘saw-tooth’ type appearance, similar to that seen in Fig. 2c. Again,

fracture of the coating occurred predominantly in two orientations, along columnar grain boundaries and

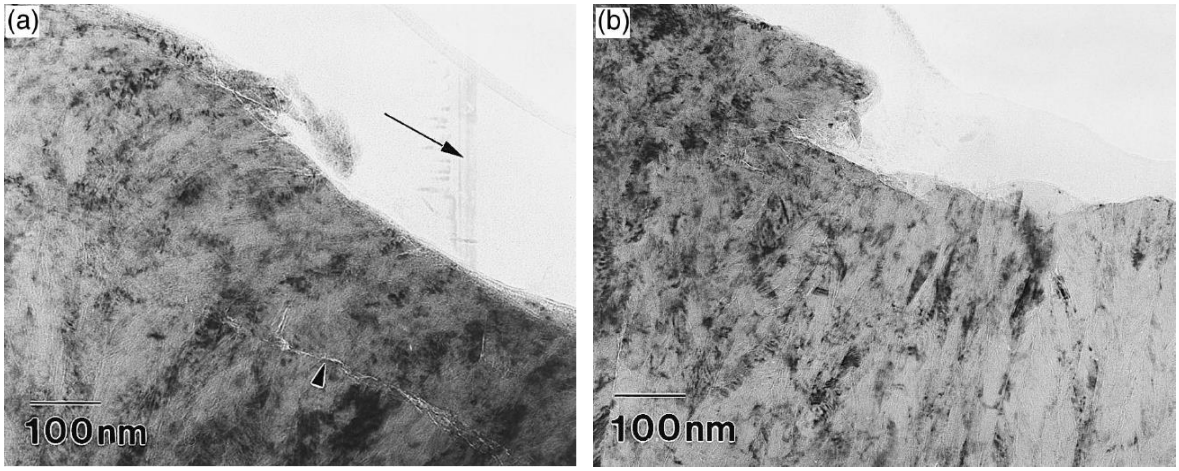

Fig. 8. Bright field TEM micrographs from a longitudinal cross-section sample of the worn TiAlCrYN monolayer showing the extreme worn surface. a. Cracking parallel to the worn surface arrowed. The cracking in this example, and several others, was at the interface between de formed and as-deposited material. b. Local detachment of a wear debris particle at a depth corresponding to the cracking in a. The sliding direction is shown by the large black arrow in each case.

Fig. 9. Bright field TEM micrograph from a longitudinal cross-section sample of the worn TiAlCrN monolayer showing the displacement of the substrate arrowed. and the cracking in the coating arrowed., similar to that seen in the multilayer coating in Fig. 5.

within ~20° of parallel to the coating surface. Cracking was mainly contained within the coating, but occasionally propagated into the substrate Fig. 10. In contrast to the absence of plastic deformation in the multilayer coating and the limited plastic deformation in the TiAlCrYN and TiAlCrN coatings, extensive plastic deformation was found at the surface of the uncoated BM2

steel Fig. 11. The martensitic structure present at the start of the test had been transformed into a predominantly a-Fe structure, with associated deformation texture a weak{100}<110> texture.

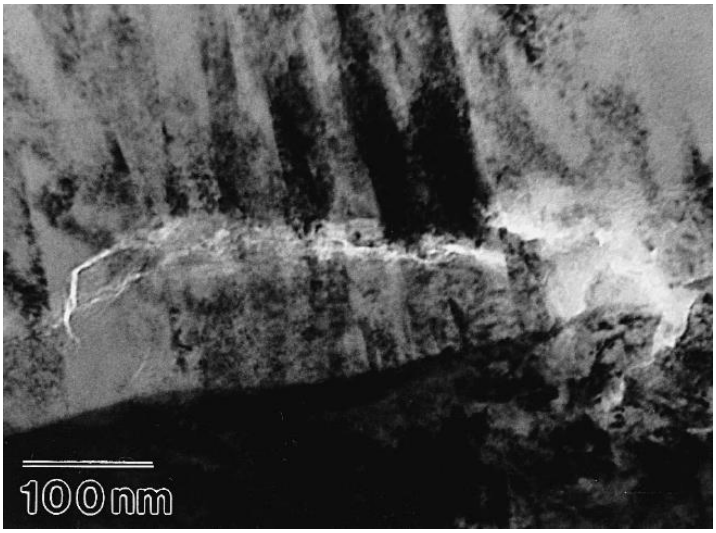

Fig. 10. Bright field TEM micrograph from a longitudinal cross-section sample of the worn TiAlCrN monolayer showing the cracking at the base of the coating.

Fig. 11. Bright field TEM micrograph from a longitudinal cross-section of the worn surface of the uncoated BM2 steel. Extensive plastic deformation is present, which has flowed around an MC carbide worn surface at the upper end of the micrograph. The arrow indicates the direction of sliding.

Subgrain size decreased as the worn surface was approached, with a minimum thickness of ~20 nm observed Fig. 12. Fig. 11 also shows the extensive plastic flow of the matrix around the

MC carbide where M denotes W, Mo, V, Cr. and the manner in which subgrain size reduces close to the MC/matrix interface.

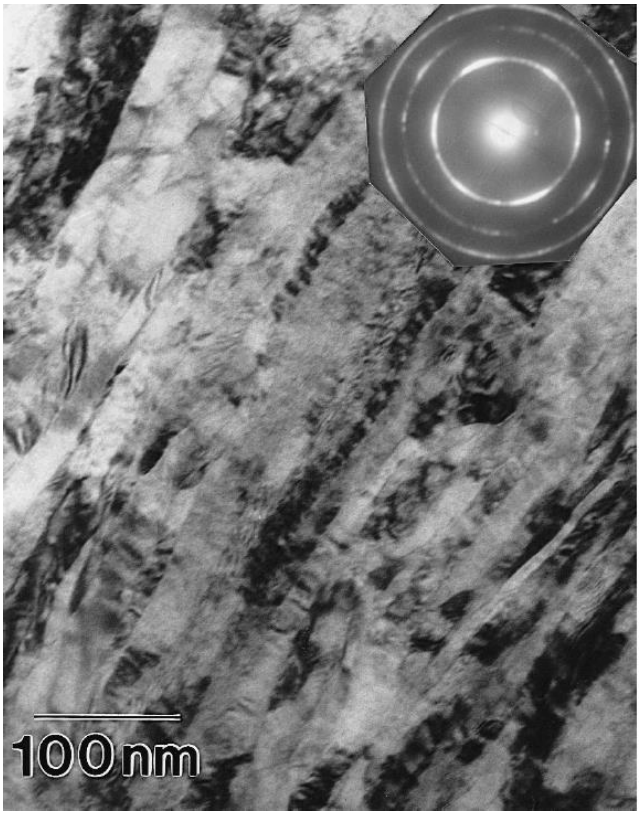

Fig. 12. Details from Fig. 11, showing a subgrain thickness of ~20 nm and the texture.

4. Discussion

All coatings provided a substantial improvement in wear rate compared with the uncoated tool steel Table 3. Of the coatings, the multilayer exhibited the lowest wear rate while the TiAlCrYN recorded the highest. These results are broadly in-line with qualitative cutting tests, which show that the multilayer coating has superior wear resistance to the first and second generation coatings.

The hardness of the TiAlCrYN, measured by knoop indentation, was lower than that obtained for the other two coatings Table 1. This was because the TiAlCrYN was thinner Table 1. than the other two coatings the test technique inevitably samples both the coating and the substrate. More detailed studies [31] have demonstrated that the true hardness of a TiAlCrYN is higher HK 2.7GPa. than the TiAlCrN, believed to be the result of greater residual stresses in the former. The higher wear rate of theTiAlCrYN compared with the TiAlCrN is believed to originate directly from the higher residual stresses, which increase the rate of spalling during sliding contact.

The trend in wear rate correlated with the extent of surface deformation observed in the TEM samples. Under the contact conditions selected, the BM2 tool steel exhibited extensive surface deformation. The contact stresses and flash temperatures were sufficient to transform

the hard martensitic structure present before testing to a heavily deformed a-Fe structure. The same conditions induced minor deformation in the TiAlCrYN and TiAlCrN coatings and no deformation in the TiAlN/CrN multilayer. There has been considerable debate as to the origin of the very high hardness values of the 'superlattice' multilayer coatings [32–37]. While the precise origin is controversial many theories have been proposed, for example, elastic modulus effects [32], alternating stress fields [33], the difference in dislocation line energy between the layers [34–37] and coherency strains [37], Hall–Petch effect [38].,it is clear that dislocation flow is severely retarded by the multilayer structure compared with the monolithic counterparts. The current TEM observations are in accord with this view. The layer structure provides a useful microstructural marker that would allow the presence of plastic deformation at the surface to be readily detected. Even in the outer few nm, the superlattice structure was retained and showed no obvious distortion. It should be emphasized that dislocation flow in a hard tool steel such as the BM2used here requires high contact stresses and the presence of such extensive plastic deformation Figs. 11 and 12.demonstrates the severity of the contact conditions.

The deformation at the surface of the monolayer coating was clearly detrimental to its wear response. Bending of the structure in the direction of sliding resulted in surfaces palling. Detachment of the wear debris particles occurred when cracks parallel to the worn surface intercepted a crack perpendicular to the worn surface usually along a columnar grain boundary. which was opened up as a result of the bending action.

Material loss in the early stages of wear of the TiAlN/CrN multilayer appeared to occur by a fundamentally different mechanism to that of the monolayer coatings. Fine scale detachment occurred by delamination of ~8 nm of material, corresponding to only a 1–3 TiAlN and CrN layers. The scale of this delamination was therefore substantially less than that observed with the mono-layer coating Fig. 8., in line with the wear rate data Table 3. Interestingly, the cracking did not appear to propagate along the layer interface. Moreover, the multilayer structure appeared to extend up to the point of delamination, indicating that surface temperatures were insufficient to give appreciable diffusion between the layers isothermal holds at ~750°C are known to induce sufficient diffusion to break down the multilayer structure[14].

The spalling and delamination shown in Figs. 4 and 8 was on a scale that would not be detected in the SEM. Nevertheless, the SEM observations indicated that failure of the coating was preceded by a mm scale spalling within the coating e.g., Fig. 1., and that locally high concentrations of spalling was a mechanism by which the counterface penetrated the coating. Observations of spalling in 1st and 2nd generation coatings are common e.g., Refs.[11,39]. Regrettably, the TEM specimens taken from the early stages of wear prior to penetration. did not reveal macroscopic cracking. Nevertheless, the morphology of the spalling Fig. 1. correlated closely with the modes of cracking observed in Figs. 5 and 9. Two types of cracking appeared to be responsible for material loss. First, pre-existing cracks along columnar grain boundaries increased in number and length as a result of the wear process, shown schematically in Fig. 13. Additional cracking occurred within the columnar grains. However, since these cracks were perpendicular to the sliding direction, they do not, on their own, lead to material loss. Secondly, cracking was developed during the wear process with an orientation within approximately ~20°

to the coating surface. These cracks tended to form initially within a single columnar grain, but propagation across columnar grains and intersection with the columnar boundary cracks provided a potent source of wear debris liberation Figs. 1 and 13. Interestingly, such cracking was constrained within the coating and did not occur at the coating-substrate interface. This

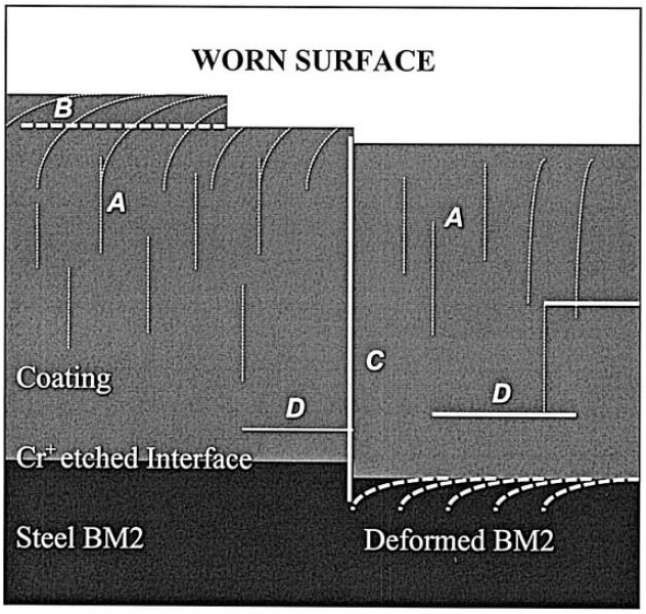

Fig. 13. Schematic of the cracking and deformation mechanisms in the coatings.

demonstrates the effectiveness of the Cr etch used at the start of the coating process to develop a strong bond.

Macroscopic cracking of the coating indicated the onset of coating failure. The present TEM observations, taken just prior to coating loss, indicated that this cracking resulted directly from plastic deformation in the substrate, leading to a strain discontinuity between coating and substrate, and therefore gross failure of the coating.

Once the coating was lost in any place, or its thickness severely reduced by local spalling, contact with the substrate occurred i.e., penetration of the coating. At this point, the wear of the coating at the edge of the wear scar proceeded rapidly, as a result of severe cracking within the coating Fig. 2. Plastic deformation within the substrate resulted in a significant strain discontinuity between coating and substrate and therefore accelerated detachment rates, in a similar manner to that observed in Figs. 5 and 9.This is in contrast to the early stages of sliding where nodeformation was found in the substrate material.

5. Conclusions

The wear rate of the TiAlN/CrN multilayer $2.58x10^{-5}mm^3/m$. was lower than that of the monolayers $3.98x10^{-5}\ mm^3/m$ for the TiAlCrN and $4.32x10^{-5}\ mm^3/m$ for the TiAlCrYN, all of which were substantially better than the uncoated BM2 substrate $6.1x10^{-4}\ mm^3/m$.

The wear rate correlated qualitatively with the hardness of the materials.

During the initial stages of sliding, wear was by a fine-scale mechanism: ~8 nm for the multilayer and ~200 nm for the monolayer. Spalling progressively occurred within the coating which ultimately resulted in penetration of the coating by the counterface. Once the substrate was exposed, accelerated wear of the coating occurred, associated with severe cracking at the edge of the wear scar.

Extensive plastic deformation was observed at the surface of the uncoated BM2 steel. Limited plastic deformation at the outer ~200 nm was found at the surfaces of the TiAlCrYN and TiAlCrN, and wear occurred by spalling of the deformed layer. No evidence of plastic deformation was found at the surface of the TiAlN/CrN multilayer.

Fine scale delamination was observed at the surface of the TiAlN/CrN multilayer, on a ;8 nm scale, but the cracking did not propagate along the TiAlN/CrN layers.

Spalling resulted from coalescence of cracks running approximately parallel to the worn surface and cracks running along columnar grain boundaries. No significant cracking was found at the coating-substrate interface.

Coating failure resulted from plastic deformation in the substrate that induced cracking in the coating as a result ofthe strain discontinuity between coating and substrate.

Acknowledgements

QL acknowledges the Joint Studentship of the University of Sheffield and Sheffield Hallam University for financial support of the experimental work. The authors wish to thank Drs. Donohue, Wadsworth and Smith and other members in the Surface Engineering Group at the Materials Research Institute, Sheffield Hallam University, who helped in the production of the sample, and Ms Bussey of Sheffield University who helped with the XTEM sample preparation and observation.

References

[1] G.S. Fox-Robinovich, A.I. Kovalev, S.N. Afanasyev, Wear 2011996. 38.

[2] F.G Kennedy, L. Tang, in: D. Dowson Ed., Tribo. Series 17: Mechanics of Coatings, Elsevier, 1990, p. 409.

[3] W.D. Sproul, Surf. Coat. Technol. 33 1987. 133.

[4] R.L. Hatschek, Amer. Machinists 129 1983. 1.

[5] G. Hakansson, L. Hultman, J.E. Sundgren, J.E. Greene, W.-D. Munz, Surf. Coat. Technol. 48 1991. 51.

[6] W.-D. Munz, J. Vac. Sci. Technol. A 4 1986. 2717.

[7] O. Knotek, H. Bo¨hmer, T. Leyendecker, J. Vac. Sci. Technol. A 41986. 2696.

[8] H. Ichimura, A. Kawana, J. Mater. Res. 8 1993. 1093.

[9] L.A. Donohue, I.J. Smith, W.-D. Munz, I. Petrov, J.E. Greene, Surf.Coat. Technol. 94–95 1997. 226.

[10] F.D. Lai, J.K. Wu, Surf. Coat. Technol. 88 1996. 183.
[11] Y.L. Su, S.H. Yao, Z.L. Leu, C.S. Wei, C.T. Wu, Wear 213 1997.165.
[12] W.-D. Munz, Werkstoffe und Korrosion 41 1990. 753.
[13] L.A. Donohue, W.-D. Munz, D.B. Lewis, J. Cawley, T. Hurkmans, T. Trinh, I. Petrov, J.E. Greene, Surf. Coat. Technol. 93 1997. 69.
[14] I Wadsworth, I.J. Smith, L.A. Donohue, W.-D. Munz, Surf. Coat. Technol. 94–95 1997. 315.
[15] U. Helmersson, S. Todorova, S.A. Barnett, J.-E. Sungren, L.C. Markert, J.E. Greene, J. Appl. Phy. 62 1987. 481.
[16] W.D. Sproul, J. Vac. Sci. Technol. A 12 1994. 1595.
[17] S. Kadlec, J. Musil, W.-D. Munz, J. Vac. Sci. Technol. A 8 3.1990. 1318.
[18] W.-D. Munz, D. Schulze, F.J. Hauzer, Surf. Coat. Technol. 501992. 169.
[19] W.-D. Munz, Surf. Coat. Technol. 49 1991. 161.
[20] W.-D. Munz, I.J. Smith, L.A. Donohue, A.P. Deeming, P. Halstead, Proc. 1st French German Conf. on High Speed Machining, Metz, France, June 1997, p. 173.
[21] K. Holmberg, A. Matthews, Tribology Series, XX, Coatings Tribology, Properties, Techniques and Applications in Surface Engineering, Elsevier, 1994, p. 69.
[22] C. Perrin, W.M. Rainforth, Wear 181–183 1995. 312.
[23] W.M. Rainforth, R. Stevens, J. Mater. Res. 13 1998. 406.
[24] W.M. Rainforth, J. Nutting, R. Stevens, Philos. Mag. A 66 1992.621.
[25] C. Perrin, W.M. Rainforth, Wear 203–204 1997. 171.
[26] W.M. Rainforth, R. Stevens, Wear 162–164 1993. 322.
[27] D.A. Rigney, M.G.S. Naylor, R. Divakar, L.K. Ives, Mater. Sci. Eng. 81 1986. 409–425.
[28] D.A. Hughes, D.B. Dawson, J.S. Korellis, L.I. Weingarten, Wear181–183 1995. 458.
[29] Q. Luo, W.M. Rainforth, I. Wadsworth, L.A. Donohue, W.-D. Munz, Surf. Coat. Technol., in press.
[30] I Wadsworth, D.B. Lewis, G. William, J. Mater. Sci. 31 1996.5907.
[31] D.B. Lewis, L.A. Donohue, W.-D. Munz, A.K. Kuˇsel, V. Valvoda, C. Blomfield, ICMCTF 1998, San Diego, USA, Surf. Coat. Technol., in press.
[32] T. Hurkmans, T. Trinh, D.B. Lewis, J.S. Brooks, W.-D. Munz, Surf.Coat. Technol. 76 1995. 159.
[33] J.W. Cahn, Acta Metall. 11 1963. 1274.
[34] J.C. Koehler, Phys. Rev. B 2 1970. 547.
[35] S.L. Lehoczky, J. Appl. Phy. 49 1978. 5479.
[36] S.L. Lehoczky, Phys. Rev. Lett. 41 1978. 1814.
[37] M. Shinn, L. Hultman, S.A. Barnett, J. Mater. Res. 7 1992. 901.
[38] P.M. Hazzledine, S.I. Rao, Mater. Res. Soc. Symp. Proc. 434 1996.135.
[39] M. Scholl, Wear 203–204 1997. 57.